

Communication-Efficient MARL for Platoon Stability and Energy-efficiency Co-optimization in Cooperative Adaptive Cruise Control of CAVs

Min Hua, Dong Chen, Kun Jiang, Fanggang Zhang, Jinhai Wang, Bo Wang, Quan Zhou, and Hongming Xu

Abstract—Cooperative adaptive cruise control (CACC) has been recognized as a fundamental function of autonomous driving, in which platoon stability and energy efficiency are outstanding challenges that are difficult to accommodate in real-world operations. This paper studied the CACC of connected and autonomous vehicles (CAVs) based on the multi-agent reinforcement learning algorithm (MARL) to optimize platoon stability and energy efficiency simultaneously. The optimal use of communication bandwidth is the key to guaranteeing learning performance in real-world driving, and thus this paper proposes a communication-efficient MARL by incorporating the quantified stochastic gradient descent (QSGD) and a binary differential consensus (BDC) method into a fully-decentralized MARL framework. We benchmarked the performance of our proposed BDC-MARL algorithm against several non-communicative and communicative MARL algorithms, e.g., IA2C, FPrint, and DIAL, through the evaluation of platoon stability, fuel economy, and driving comfort. Our results show that BDC-MARL achieved the highest energy savings, improving by up to 5.8%, with an average velocity of 15.26 m/s and an inter-vehicle spacing of 20.76 m. In addition, we conducted different information-sharing analyses to assess communication efficacy, along with sensitivity analyses and scalability tests with varying platoon sizes. The practical effectiveness of our approach is further demonstrated using real-world scenarios sourced from open-sourced OpenACC.

Index Terms—Connected and automated vehicles, multi-agent deep reinforcement learning, cooperative adaptive cruise control

I. INTRODUCTION

COOPERATIVE adaptive cruise control (CACC) is a milestone technology in achieving high-level autonomous driving as it provides a sensor-reach platform with high-level computing resources for advanced AI methods [1]. By enabling coherent communication among connected and autonomous vehicles (CAVs), CACC facilitates the formulation

The work is supported in part by the Fundamental Research Funds for the Central Universities (22120240223), by the EPSRC (EP/I00930X/1), and by Innovate UK (102253).

Min Hua, Fanggang Zhang, and Quan Zhou, and Hongming Xu are with the School of Engineering, University of Birmingham, Birmingham, UK. Corresponding author: Hongming Xu (h.m.xu@bham.ac.uk).

Dong Chen is with the Environmental Institute & Link Lab & Computer Science, University of Virginia, VA, USA

Kun Jiang is also with the School of Automation, Southeast University, Nanjing, China

Jinhai Wang is with Hubei Key Laboratory of Advanced Technology for Automotive Components, Wuhan University of Technology, Wuhan, China.

Bo Wang is with the Automotive New Technology Research Institute, BYD Auto, Shenzhen, China

Quan Zhou is also with the School of Automotive Studies, Tongji University, Shanghai, China

of vehicle platoon and determines the optimal velocity and spacing of the vehicle platoon to smooth traffic flow and reduce overall vehicle energy consumption [2]–[4]. Therefore, CACC is a foundational engineering platform to support the revolution of a smarter, safer, and more sustainable transportation system.

Rule-based methods, optimization-based methods, and learning-based methods were developed to achieve CACC of CAVs. Rule-based methods are simple and easy to implement but have limited adaptability in complex traffic environments. Optimization-based CACC methods were developed based on the optimal control theory (e.g., model predictive control (MPC)) to calculate the optimal velocity at each step for CAV platoons [5], [6]. Optimization-based methods demonstrated their capability in improving fuel economy and traffic efficiency in predefined driving environments [5]. However, most of the optimization-based methods were based on a assumption that the lead vehicle in a platoon maintains a constant velocity or a foreknown speed profile, limiting its effectiveness in real-world scenarios where vehicles often accelerate or decelerate randomly. On the other hand, the computational demands of the optimization-based methods are significant, making it hard to be implemented on vehicle onboard control units [7]. Compared to rule-based and optimization-based methods, learning-based methods, developed using deep learning, reinforcement learning, or deep reinforcement learning, offer greater adaptability and self-optimization capabilities. For instance, Lin et al. present a learning-based method using the Deep Deterministic Policy Gradient (DDPG) to improve control performance, reducing the episode cost by up to 5.8% compared to MPC methods [8].

Among the learning-based methods, multi-agent reinforcement learning (MARL) demonstrated its advancement over the single-agent reinforcement learning methods and other learning-based methods (e.g., imitation Learning) in many fields including industrial robots and autonomous driving [9]–[11]. MARL involves multiple agents learning to make decisions in a shared environment, optimizing their actions based on rewards. These agents can work together or compete, allowing them to solve complex tasks that require coordination and improve system performance [12]. In the development of CACC strategies using MARL, most of existing research focused on the development of learning algorithms and communication protocols. For example, Liu et al. propose an intermediate solution to improve the traffic efficiency of CAVs by avoiding congestion through coordinated behavior

controlled by a deep RL agent with an altruistic reward function [13]. Han et al. leveraged information-sharing MARL framework with safe actor-critic algorithm to improve traffic efficiency and safety using shared neighbor data with bounded error and safety guarantees [14]. However, there has been limited research integrating energy consumption optimization into the CACC framework using MARL. Energy efficiency is a critical aspect of CAV operations, especially with the need for sustainable transportation solutions.

In the realm of CACC, a fully decentralized MARL framework is proposed by practical considerations that align with the operational constraints specific to networked vehicular environments, which minimizes reliance on global observations during execution. In [15], global data collection introduces significant risks, including increased communication delays and higher failure rates, which in turn compromise system robustness. In contrast, Xie et al. propose a decentralized control protocol that relies on local neighbor information, addressing the challenges of unreliable communication and enhancing safety and stability [16]. The decentralized framework offers increased robustness by ensuring that the failure of a single vehicle does not compromise the entire network, thereby maintaining continuous system operation and safety [17]. Petrillo et al. utilize an adaptive synchronization-based control algorithm with decentralized mitigation of malicious information, ensuring robustness and resilience against various cyber threats [18]. Additionally, Du et al. introduce a decentralized model-based policy optimization framework (DMPO) to enhance data efficiency in CAV control [19]. Therefore, this framework is highly advantageous for CACC due to its scalability, robustness, and reduced latency in decision-making. From the perspective of communication protocols, there are communicative MARL methods [20], [21] and non-communicative MARL methods [22], [23]. However, for the CACC based on a decentralized MARL framework, inter-agent communication is critical for driving safety, and coordinating platoon stability [12], [24]. In [25], the heuristic or direct information-sharing method is employed to lead to inefficient communications. These types are easy to perform delayed information sharing [26].

While significant advances have been made in learning algorithms and communication protocols for traffic efficiency and safety, crucial aspects like energy efficiency and communication efficacy have been overlooked. This gap is evident in decentralized MARL frameworks, which are robust and scalable but lack energy-efficient strategies and effective communication protocols. This paper addresses this gap by introducing energy efficiency into CACC problems, enhancing communication protocols, and validating the approach with real-world scenarios. Therefore, the following contributions and novelties distinguish this paper from the existing works:

- 1) We have introduced energy efficiency into a short-term CACC problem as a decentralized MARL, designing a multi-objective reward function for energy efficiency, stability, and safety. We then benchmark the performance of our proposed MARL algorithm against several other algorithms, including both non-communicative and communicative MARL approaches.

- 2) We have integrated the quantized stochastic gradient descent (QSGD) method into our communication protocol and proposed a binary differential consensus (BDC) method to enhance the training process, improving information-sharing efficacy in various CACC scenarios. We also conduct extensive information-sharing analyses to assess the communication efficacy, along with sensitivity analyses and scalability tests with varying platoon sizes.
- 3) The practical effectiveness of our approach is further demonstrated using real-world scenarios sourced from the open-sourced OpenACC. By analyzing these real-world scenarios, we validate our model's applicability and robustness in achieving improved energy efficiency, stability, and safety in real-world CACC operations.

The remainder of the paper is organized as follows: Section II introduces the CACC problem formulation for CAVs. The MARL for the CACC scenario is established in Section III. In Section IV, the simulation results and discussion are discussed. Conclusions are drawn in Section V.

II. ARCHITECTURE OF MARL-BASED CACC FOR CAVS AND THE OPTIMIZATION PROBLEM

The multi-agent reinforcement learning system for CACC of CAVs is illustrated in Figure 1. The system includes N CAVs that are connected through vehicle-to-vehicle network. We assume that all CAVs in this study are plug-in hybrids equipped with a 70 kW internal combustion engine, two motor/generators (MG1 with a nominal power of 21 kW and MG2 with a nominal power of 135 kW), and a 20 kWh battery [27], [28]. Details of the vehicle modelling and vehicle specification can be found in [28]. However, when considering the dynamics of plug-in hybrids without focusing on energy management between two power sources, the electric motor is utilized for propulsion in a short-term condition without engaging the full capabilities of the hybrid powertrain.

Within an undirected graph $\mathcal{G}_t = (\mathcal{N}, \mathcal{E}_t)$ at each step t , agent i takes into account not only their current state but also the information \mathcal{E}_t from their neighbors (\mathcal{N}_{nei} represents the front and rear vehicle). and the states of its neighbor vehicles \mathcal{N}_{nei} . To train the MARL system, a new state representation mechanism is proposed by incorporating the long short-term memory (LSTM) network with a fully-connected (FC) neural network for the actor networks and critic networks of all learning agents. To update the \mathcal{N} critic networks effectively, the QSGD method is developed. Details of the system are described as follows:

A. Decentralized MADRL framework for CACC of CAV

In this section, we introduce the CACC problem as a model-free multi-agent MDP framework through a decentralized MARL algorithm to maintain a predefined and adjustable inter-vehicle spacing (IVS) d^* and longitudinal velocity v^* . Here, a fully decentralized MARL framework provides agents with only partial observations of the environment, concentrating mainly on the vehicles directly ahead and behind. This realistically reflects the practical constraints for each vehicle, which are limited in their ability to sense or communicate

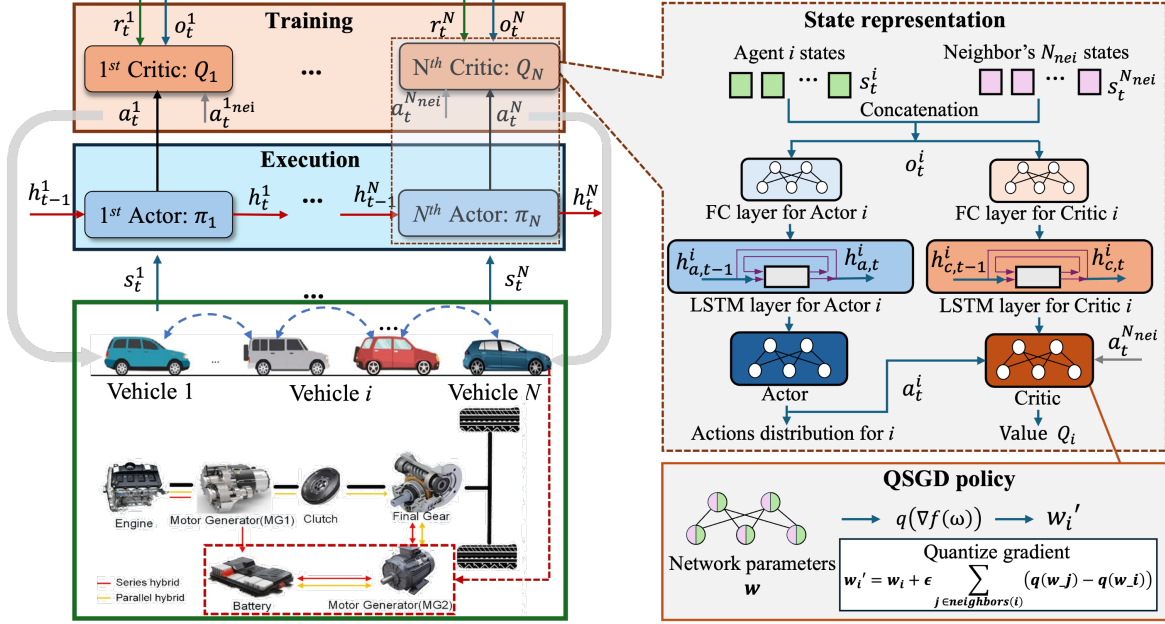


Fig. 1: The multi-agent system for CAVs

with other vehicles. Therefore, a partially observable Markov decision process (POMDP) has been formulated by the tuple $(\mathcal{S}, \{\mathcal{A}_i\}_{i \in \mathcal{N}}, P, \{R_i\}_{i \in \mathcal{N}}, \{\mathcal{G}_t\}_{t \geq 0})$. More details [29] are given as follows:

1) **State Space:** To achieve an optimal balance between accurately modeling vehicle behavior and avoiding overcomplexity, the state space \mathcal{S} is defined as $[v, v_{\text{diff}}, vh, d, u]$, specifically,

- The first state is the current normalized vehicle velocity $v = (v_{i,t} - v_{i,0})/v_{i,0}$ from time 0 to current time t , where v_i is longitudinal velocity.
- The second state is the clipped vehicle velocity difference with its leading vehicle $v_{\text{diff}} = \text{clip}((v_{i-1,t} - v_{i,t})/5, -2, 2)$, with v_i and the corresponding preceding vehicle ($i - 1$).
- The third state is the IVS-based velocity according to vehicle behavior modeling, $vh = \text{clip}((v^\circ(d_i) - v_{i,t})/5, -2, 2)$, where $v^\circ(d_i)$ represents the behavior of the i th vehicle with optimal velocity model (OVM) [30] and d_i is the IVS of each vehicle i . The formulation of OVM for the behavior of the i th vehicle is defined as follows:

$$u_i = \alpha_i (v^\circ(d_i; d^s, d^g) - v_i) + \beta_i (v_{i-1} - v_i) \quad (1)$$

$$v^\circ(d_i) \triangleq \begin{cases} 0, & \text{if } d_i < d^s, \\ \frac{1}{2} v_{\text{max}} \left(1 - \cos\left(\pi \frac{d_i - d^s}{d^g - d^s}\right) \right), & \text{if } d^s \leq d_i \leq d^g, \\ v_{\text{max}}, & \text{if } d_i > d^g \end{cases}$$

where α_i and β_i are the IVS gain and relative velocity gain respectively, highlighting how both the IVS and the relative velocity contribute to adjustments in acceleration u_i of vehicle i . Specifically, $d^s = 5$ m and $d^g = 35$ m denote the stop IVS and the IVS at full velocity for analyzing the behavior of traffic flow. Additionally, v° represents the IVS-based velocity policy. This policy function is continuous and differentiable, which is ben-

eficial for computational models and simulations in the environment of the MARL framework.

- The fourth state is the normalized IVS $d = (d_{i,t} + (v_{i-1,t} - v_{i,t}) \Delta t - d^*)/d^*$, where a sampling time Δt are given with the discretized longitudinal kinematics for each vehicle i .
- The last one is the normalized acceleration $u = u_{i,t}/u_{\text{max}}$, where u_{max} is the maximum acceleration.

By normalizing and clipping the values, the model ensures that the state variables remain within practical bounds, enhancing the model's stability and predictability in handling diverse driving scenarios.

2) **Action Space:** In the defined CACC problem, the action space $\{\mathcal{A}_i\}_{i \in \mathcal{N}}$ is straightforwardly related to the longitudinal control. According to Eq. 1, the OVM control behavior is affected by two critical hyperparameters: IVS gains α , relative velocity gain β . Thus, these values are chosen from a predefined set comprising four levels: $\{(0, 0), (0.5, 0), (0, 0.5), (0.5, 0.5)\}$. Subsequently, the longitudinal action is calculated by Eq. (1). The selection of four discrete sets of parameters for OVM within a MARL framework is driven by the goal of balancing simplicity, computational efficiency, and the capacity to model a range of driving behaviors for longitudinal vehicle control. These distinct parameter sets simplify the exploration space for the RL, enabling an efficient search through potential actions to optimize driving performance.

B. Co-optimization of platoon stability and energy efficiency

1) **Reward function:** The collective objective is to train the agents toward these desired behaviors. So the multi-objective reward $\{R_i\}_{i \in \mathcal{N}}$ for the i th agent is designed as follows:

$$R_i = w_1 (d_i - d^*)^2 + w_2 (v_i - v^*)^2 + w_3 u_i^2 + w_4 (2d_s - d_i)_+^2 + w_5 P_i \quad (2)$$

where w_1, w_2, w_3, w_4 , and w_5 are the weighting coefficients. This multi-objective reward design is conducted to achieve

a trade-off between performance efficiency, driving comfort, safety, and energy savings in the CACC system. P_i is the power consumption of the electric motor of each vehicle, where a polynomial-based, differentiable approximation of an energy consumption model [31] is calculated as follows:

$$\begin{aligned} P_i &= T_i \cdot \omega_i \cdot \eta_i^{-k} \\ T_i &= F_i \cdot R \end{aligned} \quad (3)$$

where T_i represents the motor torque of each vehicle, ω_i is the rotational velocity of the motor for each vehicle, and η_i is the efficiency of electric-mechanical conversion. The k indicates the operational mode. $k = 1$ denotes the driving model while $k = -1$ denotes regenerative braking mode. The driving force of each vehicle, F_i , can be calculated by

$$\begin{aligned} F_i(t) &= mgf \cos \alpha + \frac{1}{2} \rho P_i(t) = F_i(t) \cdot v_i \\ T_i(t) &= F_i(t) \cdot R \end{aligned} \quad (4)$$

where m is the vehicle mass; g is the gravity acceleration; f is the rolling resistance coefficient; ρ is the air density; A_f is the front area of the vehicle; C_d is the aerodynamic drag coefficient; R is the wheel radius; α is the road slope. The critical parameters can be found in [28]. To simplify the calculation and calibration, the vehicle energy consumption, $P_i(v_i, u_i)$, is formulated as a function of vehicle velocity v_i and acceleration u_i as in [32],

$$P_i(v_i, u_i) = \sum_{k=0}^4 \sum_{j=0}^4 p_{kj} \cdot v_i^k \cdot u_i^j \quad (5)$$

where p_{kj} is the polynomial coefficient determined by fitting as shown in Figure 2. In this work, each vehicle equipped with the CACC is considered to have identical capabilities and physical characteristics. The inclusion of the real energy model reveals that the CACC not only regulates vehicle velocity and inter-vehicle spacing (IVS) but also actively manages the powertrain to improve fuel economy and energy efficiency.

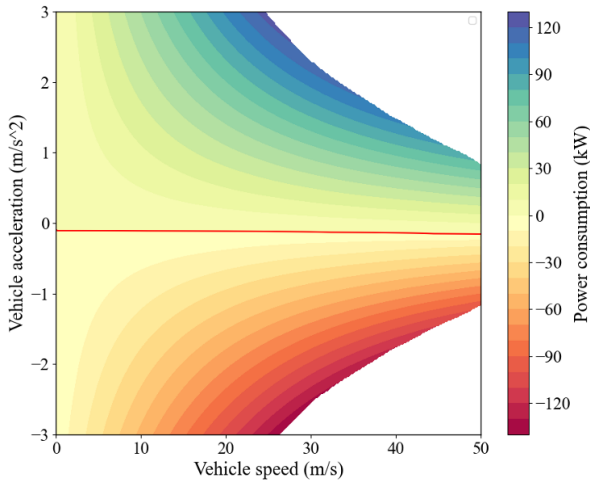


Fig. 2: Contour plot of the fitted energy consumption model with respect to vehicle velocity and acceleration.

Further, if the IVS is less than twice the stop IVS d_s , preventing collisions and ensuring the safety of the vehicle

platoon. Here, the "+" in the reward function indicates that a penalty is applied only when the d_i falls below twice the d_s , functioning similarly to a Rectified Linear Unit (ReLU) by activating the penalty under specific conditions; if the IVS $d_i \leq 1$ m, the substantial penalty of 1000 serves as a strong deterrent against behaviors that could lead to collisions, effectively terminating the training episode to guarantee safety.

2) **Transition Probabilities:** Based on the model-free MARL, we do not assume any prior knowledge of this transition probability P while developing our MARL algorithm.

III. COMMUNICATION-EFFICIENT MADRL FOR CACC

A. Decentralized Multi-agent MDP problem

The system consists of N agents, indexed by $\mathcal{N} = [N]$, interacting within a shared environment. They communicate via a dynamic network represented as $\mathcal{G}_t = (\mathcal{N}, \mathcal{E}_t)$ at each step t . The multi-agent Markov decision process (MDP) in this networked environment is defined by the tuple $(\mathcal{S}, \{\mathcal{A}_i\}_{i \in \mathcal{N}}, P, \{R_i\}_{i \in \mathcal{N}}, \{\mathcal{G}_t\}_{t \geq 0})$, where \mathcal{S} is the global state space and \mathcal{A}_i is the action space for each agent i . The local reward function for each agent i is $R_i : \mathcal{S} \times \mathcal{A} \rightarrow \mathbb{R}$, and $P : \mathcal{S} \times \mathcal{A} \times \mathcal{S} \rightarrow [0, 1]$ is the state transition probability function. Each agent i chooses its action a_i based on the local policy $\pi^i : \mathcal{S} \times \mathcal{A}_i \rightarrow [0, 1]$, leading to a joint policy $\pi(s, a) = \prod_{i \in \mathcal{N}} \pi^i(s, a_i)$. A fully decentralized framework is characterized by the fact that the reward is received locally and the action is executed individually by each agent. The policy for each agent i is parameterized by π_{θ^i} with θ^i over Θ^i , where $\Theta = \prod_{i=1}^N \Theta^i$ by packing the parameters together as $\theta = [(\theta^1)^T, \dots, (\theta^N)^T]^T \in \Theta$. Thus, the joint policy then becomes $\pi_{\theta}(s, a) = \prod_{i \in \mathcal{N}} \pi_{\theta^i}(s, a_i)$. We assume that the Markov chain $\{s_t\}_{t \geq 0}$ is irreducible and aperiodic under any π_{θ} , with the stationary distribution denoted by d_{θ} . Additionally, the Markov chain of the state-action pair $\{(s_t, a_t)\}_{t \geq 0}$ has a stationary distribution $d_{\theta}(s) \cdot \pi_{\theta}(s, a)$ for any $s \in \mathcal{S}$ and $a \in \mathcal{A}$. Furthermore, the collective objective of the agents is to collaboratively find a policy π_{θ} that maximizes the globally averaged long-term return over the network based solely on local information, formalized as:

$$\begin{aligned} \max_{\theta} J(\theta) &= \lim_T \frac{1}{T} \mathbb{E} \left(\sum_{t=0}^{T-1} \frac{1}{N} \sum_{i \in \mathcal{N}} r_{t+1}^i \right) \\ &= \sum_{s \in \mathcal{S}, a \in \mathcal{A}} d_{\theta}(s) \cdot \pi_{\theta}(s, a) \cdot \bar{R}(s, a) \end{aligned} \quad (6)$$

where $\bar{R}(s, a) = N^{-1} \cdot \sum_{i \in \mathcal{N}} R^i(s, a)$ is the globally averaged reward function. The global relative action-value function $Q_{\theta}(s, a)$ and state-value function $V_{\theta}(s)$ are defined as $Q_{\theta}(s, a) = \sum_t \mathbb{E}[\bar{r}_{t+1} - J(\theta) \mid s_0 = s, a_0 = a, \pi_{\theta}]$ and $V_{\theta}(s) = \sum_{a \in \mathcal{A}} \pi_{\theta}(s, a) Q_{\theta}(s, a)$ respectively. Furthermore, the advantage function can be defined as $A_{\theta}(s, a) = Q_{\theta}(s, a) - V_{\theta}(s)$.

In this paper, the typical deployment scenario for CACC involves extensive offline training and testing to address safety and efficiency concerns and avoid online learning. Kuutti et al. emphasize the effectiveness of extensive offline training in

reducing deployment risks and enhancing system reliability [21]. Hence, a decentralized MDP framework ensures that each vehicle, acting as an autonomous control agent, primarily relies on local information and communicates within a limited neighborhood. This approach effectively addresses the challenges of partial observability and non-stationarity in a multi-agent environment by allowing each vehicle to enhance responsiveness and adaptability but also ensures that training, although decentralized, happens offline with global information available in batches during the training phase.

B. Communication protocol design

Quantified stochastic gradient descent (QSGD) method is a family of compression schemes with convergence guarantees and practical performance, this method balances communication bandwidth and convergence time by adjusting the number of bits sent per iteration, maintaining convergence even with reduced precision [33]. Significantly, the decentralized framework operates without the need for a centralized controller. However, it operates under the assumption that all agents are homogeneous, possessing identical characteristics. While this assumption simplifies the structural complexity of the problem, it fails to capture the inherent diversity among individual agents, especially for CACC. To tackle this issue, we introduce a difference update strategy that promotes a balance between individual learning and the collaborative influence by neighboring agents. Then, a binary differential consensus (BDC) method is presented, where agents first quantize their weights and then update their weights based on the quantized differential weights between themselves and their neighbors. Therefore, the update rule is described as:

$$w'_i = w_i + \epsilon \sum_{j \in \text{neighbors}(i)} (q(w_j) - q(w_i)) \quad (7)$$

where w'_i is the updated weight for agent i . w_i is the current weight of the agent i before the update. ϵ is a small positive scalar that scales the update magnitude. $q(w_j)$ and $q(w_i)$ are the quantized weights of neighbor agent j and agent i , respectively, mapped to -1, 0, 1 based on the sign of the weight. The sum is taken over all neighbors j of agent i , as defined by the neighbor mask.

We utilize quantization to potentially reduce communication overhead while still achieving consensus through differential updates. To mitigate the impact of quantization errors, QSGD often incorporates mechanisms like error accumulation (also known as error feedback), which means the quantization error from one iteration (i.e., the difference between the quantized gradient and the actual gradient) is carried over to the next iteration. This error feedback helps compensate for the quantization errors over time, allowing for more accurate updates despite the initial loss of information. The update strategy is given in Algorithm 1.

In the CACC scenario, by transmitting only three possible values for each gradient component, the system minimizes the amount of data exchanged between vehicles, preserving bandwidth for critical vehicular communications. Since smaller messages mean quicker transmissions, which is crucial for real-time or near-real-time applications like CACC where

Algorithm 1: The gradient descent algorithm with gradient encoding

```

1 Data: Parameter vector  $w$ 
2 Procedure: Gradient Descent
3 for each iteration  $t$  do
4   Quantize gradient:  $q(\nabla f(w)) \leftarrow$  Quantize
    $(\nabla f(w))$ ;
5   Apply gradient  $w \leftarrow w - \epsilon_t q(\nabla f(w))$ 
6 end

```

timely updates can impact system performance and vehicle safety. With less dependency on the bandwidth, the system can scale more effectively, accommodating more vehicles without proportional increases in communication overhead. While it introduces some challenges in terms of convergence and accuracy, these can be managed through strategic implementations like error feedback. This makes it a effective technique for distributed systems in high-demand, bandwidth-constrained environments such as CACC scenario.

IV. EXPERIMENT SETUPS

In this section, we evaluate the BDC-MARL framework across various CACC scenarios. Initially, our approach is compared with several leading-edge MARL strategies. Then we explore the efficacy of diverse information-sharing methods. Concurrently, we investigate the effects of different platoon sizes. Finally, the proposed algorithm is applied to scenarios derived from real-world OpenACC data.

A. General setups for the learning agents

The network architecture comprises a single fully-connected input layer for processing state information and an LSTM layer tasked for message extraction, all with hidden layers containing 64 neurons. An orthogonal initializer is utilized to optimize the network parameters during training. Training is conducted over 6×10^5 steps, utilizing a discount factor of $\gamma = 0.99$, an actor learning rate of 5.0×10^{-4} , and a critic learning rate of 2.5×10^{-4} . In the reward function, hyperparameters w_1, w_2, w_3, w_4 , and w_5 in the reward function are set to -1.0, -1.0, -0.1, -5.0, and -10, respectively, with significant emphasis on penalizing scenarios that feature inadequate safe IVS distances. To enhance generalization, each model undergoes training three times using distinct random seeds on a Ubuntu 18.04 server with a NVIDIA RTX 3080.

B. Real-world driving scenario extraction

The real-world scenarios are from an open-access database involving vehicles with adaptive cruise control (ACC) systems provided by the Joint Research Centre (JRC) of the European Commission (EC) [34]. The dataset used in this paper is collected at the ZalaZONE from 10 commercially-available vehicles with tunable ACC settings. The data was captured using INVENTURE (Race Logic VBOX) equipment, U-blox 9, and the Tracker App, with sensor data from these devices fused and interpolated at a frequency of 10 Hz.

The real-world driving scenarios are generated for the testing in this paper based on the Dynamic Platform. The Dynamic Platform focuses on the vehicles' response to such perturbations in a controlled environment. This includes a

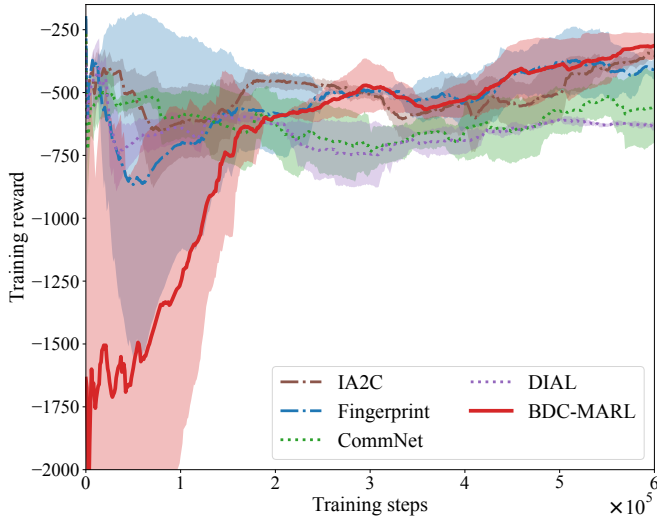


Fig. 3: The comparison with different methods

rapid deceleration followed by an acceleration back to the original velocity. Three groups are selected and extracted respectively from three typical datasets (dynamic_part1, dynamic_part2, dynamic_part9) from timestamps (316s – 376s, 450s – 510s, 473s – 533s).

V. RESULTS AND DISCUSSION

In this section, we evaluate the BDC-MARL framework across various CACC scenarios. Initially, our approach is compared with several leading-edge MARL strategies. Then we explore the efficacy of diverse information-sharing methods. Concurrently, we investigate the effects of different platoon sizes. Finally, the proposed algorithm is applied to scenarios derived from real-world OpenACC data.

A. Co-optimization Performance with State-of-the-art MARL

To demonstrate the effectiveness of the proposed method, we compare with several state-of-the-art MARL algorithms, which include both non-communicative and communicative approaches. Specifically, IA2C [22] employs an independent learning strategy, while FPrint [23] integrates neighboring policies into its inputs, both of which are non-communicative methods. In contrast, DIAL [20] and CommNet [35] implement learnable communication protocols that allow for the inclusion of additional information from neighboring agents, such as states or policy details, which necessitates a higher communication bandwidth. All the algorithms compared utilize the same deep neural network architecture.

A comparative learning progress through training curves for the various MARL algorithms are described as shown in Figure 3 and Table I. The proposed BDC-MARL outperforms other algorithms, starting with a higher initial reward and steadily increasing performance. Despite early fluctuations, it maintains a higher reward throughout training, indicating extensive strategy exploration before stabilizing. This thorough exploration can lead to more optimal policies. After the training phase, the evaluation phase for each algorithm included 50 distinct trials, each initiated with different initial conditions to

ensure a thorough and varied testing environment, as shown in Table II. It achieved significantly higher rewards without compromising power consumption efficiency. Although it shows slightly higher standard deviations in some metrics, this suggests an adaptive strategy. All algorithms effectively prioritized safety, with consistently low or zero collisions.

Figure 4 compares the performance of 8 vehicles using different MARL algorithms, including I2AC, CommNet, and BDC-MARL, based on IVS, velocity, acceleration, and power consumption over time. Divergences in some vehicles with I2AC (e.g., Vehicle 2 and 4) and CommNet (e.g., Vehicle 1) suggest challenges in information sharing and coordination. Effective communication is crucial for synchronizing actions and maintaining uniform IVS and velocity in MARL systems like CACC. The I2AC method’s divergences may indicate lagging communication channels, while CommNet’s velocity fluctuations suggest inefficient use of communicated information. These issues imply potential communication latency or protocols preventing agents from aligning actions effectively in dynamic tasks. Conversely, BDC-MARL’s convergence towards the desired IVS and velocity with less variability indicates a more efficient communication strategy, enabling better coordination and faster adaptation to achieve goals.

B. Communication Efficiency of MARL on CACC

Using different information-sharing methods in CACC systems is crucial because each method offers unique benefits in various traffic scenarios and communication environments. For example, a broadcast method ensures all vehicles have the same information, promoting consistent behavior, enhancing safety, and preventing collisions. This is achieved with weight averaging consensus (WAC)-MARL, where each agent’s weights are averaged with its neighbors. Alternatively, directed information sharing, which communicates with neighbors, efficiently relays information in both directions within a platoon. This approach uses differential consensus-enhanced adjustment (DCEA)-MARL, adjusting each agent’s weights by adding a weighted difference between the neighbors’ weights and its own. The term $w'_i = w_i + \epsilon \sum_{j \in \text{neighbors}(i)} (w_{j+1} - w_{i+1})$ captures the essence of this update mechanism, where an epsilon factor ϵ is the scale factor. The selective sharing, such as the proposed method BDC-MARL, is more appropriate when the bandwidth is limited or when too much information could overwhelm the processing capabilities of individual agents, leading to increased reaction times or errors. Hence, Figure 5 presents a comparison of learning curves, highlighting the superior performance of the BDC-MARL method against the other two.

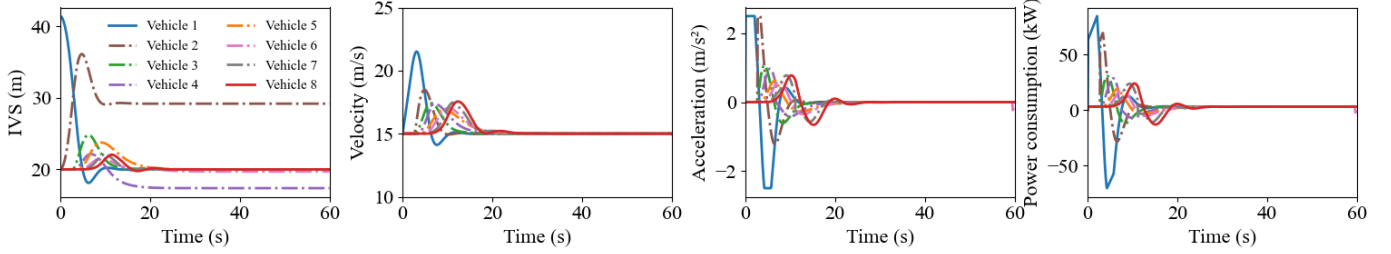
While BDC-MARL exhibits some mid-training variability, it ultimately achieves the highest rewards, making it the most effective method for maximizing training rewards. DCEA-MARL shows good initial learning velocity and stability, ideal for scenarios where early performance is critical. WAC-MARL demonstrates steady improvement and stability, suitable for environments requiring consistent performance gains over time. After the training phase, each algorithm was evaluated on 50 seeds under varied starting conditions. The performance

TABLE I: Reward comparison with different algorithms

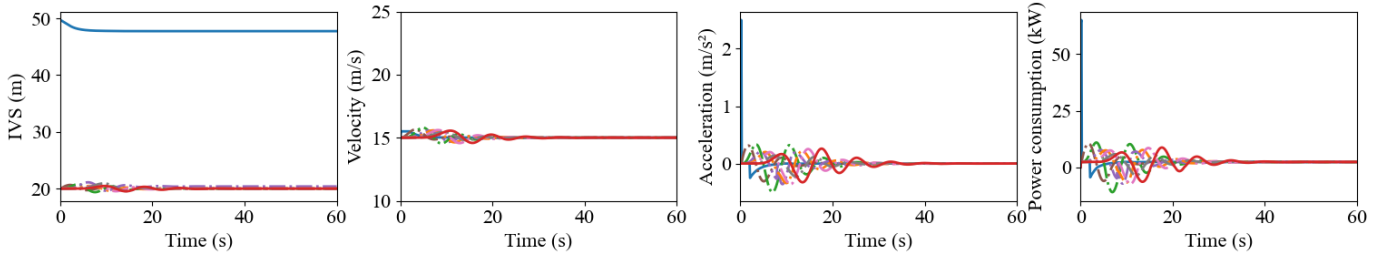
Algorithms	IA2C	Fingerprint	Commnet	DIAL	BDC-MARL
Reward value	-351.07	-409.12	-559.45	-636.19	-314.99

TABLE II: Test performance comparison with different algorithms

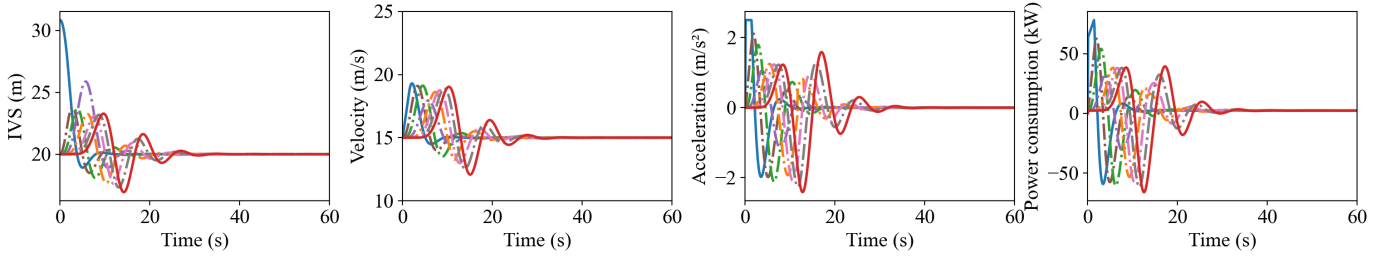
Algorithms Statistical value	IA2C		Fingerprint		Commnet		DIAL		BDC-MARL	
	Average	Std	Average	Std	Average	Std	Average	Std	Average	Std
IVS (m)	20.75	0.81	21.68	0.31	22.38	0.03	22.08	0.2	20.76	0.78
Velocity (m/s)	15.28	0.47	15.11	0.26	15.01	0.03	15.06	0.09	15.26	0.69
Acceleration (m/s ²)	0.11	0.18	0.08	0.13	0.01	0.02	0.04	0.05	0.15	0.21
Platoon power consumption (kW)	17.97	0.31	18.28	0.42	18.94	0.04	18.89	0.15	17.85	0.46
Collision number	0	0	0	0	0	0	0	0	0	0



(a) IA2C method



(b) CommNet method



(c) BDC-MARL method

Fig. 4: The performance comparison of all vehicles with typical MARL algorithms

process with all vehicles is illustrated in Figure 6. Comparing Figure 4 (c) with Figure 6, all three methods eventually converge towards a pre-designed IVS and velocity. The WAC method shows initial over-corrections in acceleration and power consumption before stabilizing. The DCEA method reaches stability quicker than the WAC method, despite initial inconsistencies in acceleration and velocity. The BDC-MARL approach quickly converges in terms of IVS and maintains a more stable velocity and acceleration pattern, due to its efficient use of limited bandwidth and information processing capabilities, preventing data overflow and response lag.

The radar chart in Figure 7 evaluates the performance of three methods using four metrics. This chart effectively

visualizes comprehensive performance through the aggregate area of each method's plot. A smaller area within the radar chart signifies a more robust overall performance, indicating a method's efficiency and effectiveness across the evaluated dimensions. Therefore, the balance across all four metrics for BDC-MARL can imply a more robust overall system performance. For IVS and velocity, all three methods show comparable performance, with their lines relatively close to the outer edge. However, in acceleration and power consumption, the BDC-MARL method is noticeably closer to the edge, indicating superior performance in these areas.

In summary, while the WAC and DCEA methods initially face oscillations, they eventually achieve consensus, promoting

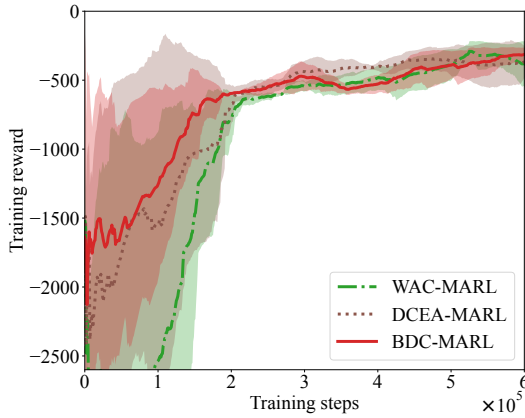


Fig. 5: The comparison with three different sharing methods

collective efficiency. However, the BDC-MARL method stands out for its quick convergence and stability, demonstrating its effectiveness in environments with limited communication resources.

C. Impact of Platooning Size on the Scalability of MARL on CACC

In CACC, the overall performance including energy efficiency, safety, and the effectiveness of communication will be affected by different vehicle sizes, since there is the propagation phenomenon in the response and communication signals.

Figure 8 shows the training curves with different sizes, ranging from a minimal arrangement (i.e., 2 AVs) to more populated configurations (i.e., 6 and 8 AVs), thereby providing a comprehensive overview of the scalability and adaptability in a variety of urban traffic scenarios, since larger vehicle sizes experience more complex effects, such as increased air resistance or more intricate behavior in a platoon. In Figure 8, we can find that Size 8 needs more sophisticated models to handle these effects effectively, which could explain a slower but steady increase in training process. In contrast, Size 2 experiences less interaction and therefore might find an optimal policy faster.

The overall test performance under 50 different trials is displayed in Figure 9. The comprehensive analysis of varying platoon sizes suggests that while larger platoons achieve fuel savings due to decreased aerodynamic drag, this does not result in a proportional increase in power consumption. Interestingly, a platoon size of 6 emerges as the most advantageous, exhibiting consistent IVS, moderate velocities, and the lowest variation in power consumption, indicative of an efficient balance between fuel efficiency and operational stability. Although larger platoons benefit from aerodynamic efficiency, they also confront the challenge of maintaining stable and safe following distances amidst dynamic traffic conditions, which is less of a concern with smaller platoons. Therefore, a platoon size of 6 is potentially optimal for achieving a harmonious balance between power efficiency, vehicle spacing stability, and the complexities inherent in managing larger numbers of closely following vehicles. More importantly, it also indicates that the presented algorithms effectively optimize platoon

dynamics, achieving fuel economy improvements without a corresponding escalation in power consumption across varying platoon sizes.

D. Co-optimization Performance Validation with Real-World Data

In this part, the different targets (the target IVS and velocity) on the performance of the presented algorithm has been conducted from the real-data scenarios extracted from OpenACC. The examination is primarily focused on analyzing three different IVS settings with the target velocity 11 m/s and the Size 4, ranging from IVS setting S (12m), M (16m), and L (20m), labelled as Group 1, Group 2, and Group 3.

Table III presents average and standard deviation values for velocity, IVS, acceleration, and total energy for vehicles in the proposed BDC-MARL algorithm and real-world OpenACC data. Here, the average velocities are close to the target velocity of 11 m/s, indicating that all strategies and groups are performing well in terms of pre-designed setting. However, there are noticeable differences in the standard deviation of IVS, showing greater variability in the OpenACC. The total energy consumption is fairly consistent across groups, since the analysis has been conducted over a short period, which might not be sufficient to capture the long-term benefits of BDC-MARL in terms of energy savings but the stability of the vehicle dynamics is improved.

VI. CONCLUSION

The paper introduces a binary differential consensus (BDC)-MARL approach to enhance system robustness and efficiency. By minimizing dependency on potentially delayed or unreliable information exchanges between vehicles, this approach optimizes individual vehicle responses to real-time traffic conditions. The main conclusions are summarized as follows::

(1) Compared with state-of-the-art algorithms, the BDC-MARL achieves the largest improvement in energy savings, up to 5.8%, with an average velocity of 15.26 m/s and an IVS of 20.76 m. In CACC scenarios, delayed messages in real-time CACC tasks hinder performance, as observed with I2AC and CommNet. In contrast, BDC-MARL demonstrates efficient communication that effectively mitigates this issue.

(2) Integrating QSGD into our communication protocol achieves stable performance and comparable energy savings across three information-sharing methods. Among them, the BDC-MARL approach rapidly converges for IVS and maintains a more stable velocity and acceleration pattern, effectively using limited bandwidth and processing capabilities to prevent data overflow and delays.

(3) A 6-vehicle platoon is optimal for balancing efficiency and stability, demonstrating the scalability in optimizing platoon dynamics for energy efficiency. Larger platoons save fuel through reduced aerodynamic drag without increasing power use proportionally.

(4) While average velocities align with the target in both BDC-MARL and OpenACC data, OpenACC exhibits greater variability in IVS due to less efficient coordination between vehicles. Despite short-term consistency in energy consumption,

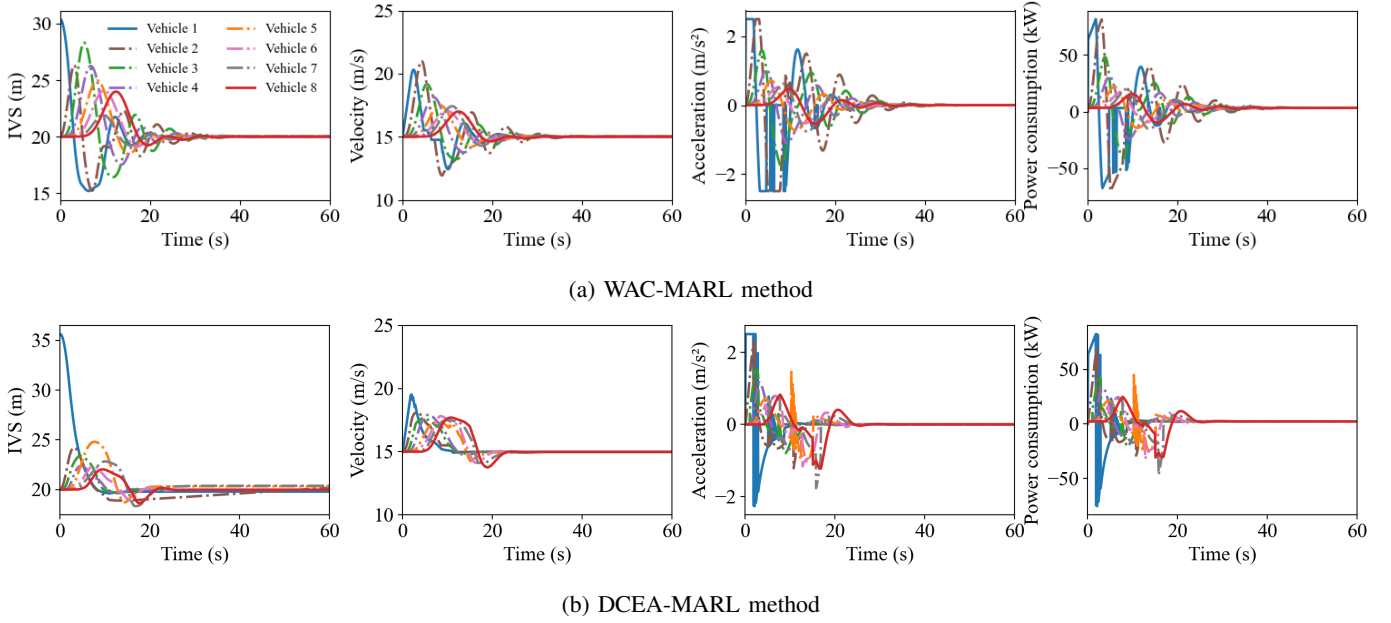


Fig. 6: The performance process of different sharing methods

TABLE III: Extraction of real-world scenarios from OpenACC

Group	Statistical Values	Method	Velocity (11 m/s)	IVS (m)	Acceleration	Total energy for all vehicles (kWh)
1 (S)	Average	OpenACC	10.81	16.96	0.01	0.11
		BDC-MARL	10.75	11.99	0	0.11
	Std	OpenACC	2.01	5.36	0.77	/
		BDC-MARL	0.73	1.37	0.23	/
2 (M)	Average	OpenACC	10.28	21.89	0.11	0.09
		BDC-MARL	10.2	16.99	0	0.09
	Std	OpenACC	2.08	3.68	0.68	/
		BDC-MARL	2.23	2.27	0.71	/
3 (L)	Average	OpenACC	10.6	25.12	0.02	0.10
		BDC-MARL	10.47	19.54	0	0.10
	Std	OpenACC	1.68	4.3	0.55	/
		BDC-MARL	1.47	2.15	0.55	/

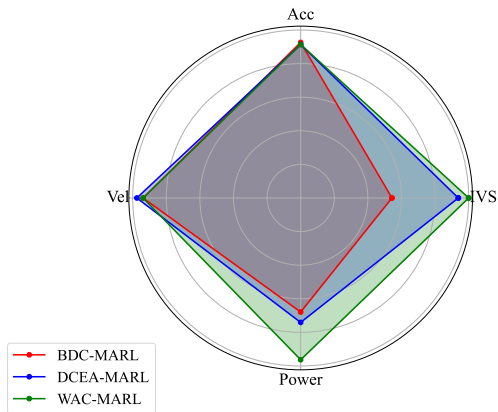


Fig. 7: The statistical comparison of different communicative methods

BDC-MARL enhances vehicle dynamics stability by leveraging robust communication protocols and optimized response strategies.

Future work will focus on extending the analysis to longer periods to better assess the long-term energy savings potential

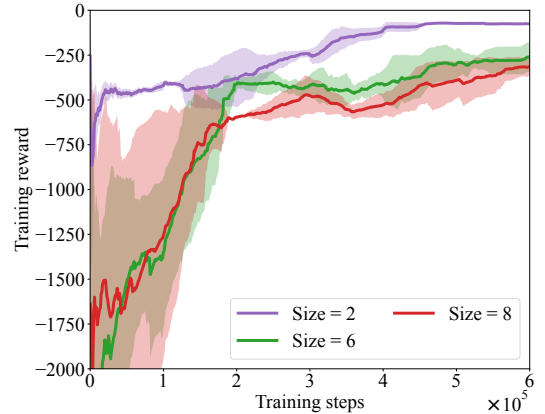


Fig. 8: The comparison with different sizes

of BDC-MARL, refining communication protocols to reduce variability in IVS, and enhance real-time coordination.

VII. ACKNOWLEDGEMENT

The work is supported in part by the Fundamental Research Funds for the Central Universities (22120240223), by the EPSRC (EP/J00930X/1), and by Innovate UK (102253).

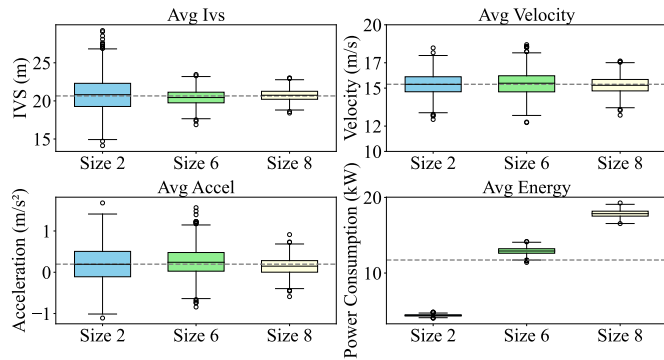


Fig. 9: The comparison with different size

REFERENCES

- W. Liu, M. Hua, Z. Deng, Z. Meng, Y. Huang, C. Hu, S. Song, L. Gao, C. Liu, B. Shuai *et al.*, "A systematic survey of control techniques and applications in connected and automated vehicles," *IEEE Internet of Things Journal*, 2023.
- S. Boddupalli, A. S. Rao, and S. Ray, "Resilient cooperative adaptive cruise control for autonomous vehicles using machine learning," *IEEE Transactions on Intelligent Transportation Systems*, vol. 23, no. 9, pp. 15 655–15 672, 2022.
- Z. Wang, G. Wu, and M. J. Barth, "Cooperative eco-driving at signalized intersections in a partially connected and automated vehicle environment," *IEEE Transactions on Intelligent Transportation Systems*, vol. 21, no. 5, pp. 2029–2038, 2019.
- C. Dai, C. Zong, D. Zhang, M. Hua, H. Zheng, and K. Chuyo, "A bargaining game-based human–machine shared driving control authority allocation strategy," *IEEE Transactions on Intelligent Transportation Systems*, 2023.
- J. Wang, Z. Jiang, and Y. V. Pant, "Improving safety in mixed traffic: A learning-based model predictive control for autonomous and human-driven vehicle platooning," *Knowledge-Based Systems*, p. 111673, 2024.
- F. Yang, H. Wang, D. Pi, X. Sun, and X. Wang, "Research on collaborative adaptive cruise control based on mpc and improved spacing policy," *Proceedings of the Institution of Mechanical Engineers, Part D: Journal of Automobile Engineering*, p. 09544070241240166, 2024.
- H. Kazemi, H. N. Mahjoub, A. Tahmasbi-Sarvestani, and Y. P. Fallah, "A learning-based stochastic mpc design for cooperative adaptive cruise control to handle interfering vehicles," *IEEE Transactions on Intelligent Vehicles*, vol. 3, no. 3, pp. 266–275, 2018.
- Y. Lin, J. McPhee, and N. L. Azad, "Comparison of deep reinforcement learning and model predictive control for adaptive cruise control," *IEEE Transactions on Intelligent Vehicles*, vol. 6, no. 2, pp. 221–231, 2020.
- B. Shuai, M. Hua, Y. Li, S. Shuai, H. Xu, and Q. Zhou, "Optimal energy management of plug-in hybrid electric vehicles through ensemble reinforcement learning with exploration-to-exploitation ratio control," *IEEE Transactions on Intelligent Vehicles*, 2024.
- M. Hua, D. Chen, X. Qi, K. Jiang, Z. E. Liu, Q. Zhou, and H. Xu, "Multi-agent reinforcement learning for connected and automated vehicles control: Recent advancements and future prospects," *arXiv preprint arXiv:2312.11084*, 2023.
- G. Chen, Z. Gao, M. Hua, B. Shuai, and Z. Gao, "Lane change trajectory prediction considering driving style uncertainty for autonomous vehicles," *Mechanical Systems and Signal Processing*, vol. 206, p. 110854, 2024.
- T. Chu, S. Chinchali, and S. Katti, "Multi-agent reinforcement learning for networked system control," in *International Conference on Learning Representations*, 2020. [Online]. Available: <https://openreview.net/forum?id=Syx7A3NFvH>
- B. Liu, W. Han, E. Wang, S. Ma, S. Xiong, C. Qiao, and J. Wang, "An efficient message dissemination scheme for cooperative drivings via multi-agent hierarchical attention reinforcement learning," in *2021 IEEE 41st International Conference on Distributed Computing Systems (ICDCS)*. IEEE, 2021, pp. 326–336.
- S. Han, S. Zhou, J. Wang, L. Pepin, C. Ding, J. Fu, and F. Miao, "A multi-agent reinforcement learning approach for safe and efficient behavior planning of connected autonomous vehicles," *IEEE Transactions on Intelligent Transportation Systems*, 2023.
- K. Zhang, Z. Yang, and T. Başar, "Decentralized multi-agent reinforcement learning with networked agents: Recent advances," *Frontiers of Information Technology & Electronic Engineering*, vol. 22, no. 6, pp. 802–814, 2021.
- S. Xie, J. Hu, Z. Ding, and F. Arvin, "Cooperative adaptive cruise control for connected autonomous vehicles using spring damping energy model," *IEEE Transactions on Vehicular Technology*, vol. 72, no. 3, pp. 2974–2987, 2023.
- H. Long, A. Khalatbarisoltani, Y. Yang, and X. Hu, "Hierarchical control strategies for connected heavy-duty modular fuel cell vehicles via decentralized convex optimization," *IEEE Transactions on Vehicular Technology*, 2023.
- A. Petrillo, A. Pescape, and S. Santini, "A secure adaptive control for cooperative driving of autonomous connected vehicles in the presence of heterogeneous communication delays and cyberattacks," *IEEE transactions on cybernetics*, vol. 51, no. 3, pp. 1134–1149, 2020.
- Y. Du, C. Ma, Y. Liu, R. Lin, H. Dong, J. Wang, and Y. Yang, "Scalable model-based policy optimization for decentralized networked systems," in *2022 IEEE/RSJ International Conference on Intelligent Robots and Systems (IROS)*. IEEE, 2022, pp. 9019–9026.
- J. Foerster, I. A. Assael, N. De Freitas, and S. Whiteson, "Learning to communicate with deep multi-agent reinforcement learning," *Advances in neural information processing systems*, vol. 29, 2016.
- S. Kuutti, R. Bowden, Y. Jin, P. Barber, and S. Fallah, "A survey of deep learning applications to autonomous vehicle control," *IEEE Transactions on Intelligent Transportation Systems*, vol. 22, no. 2, pp. 712–733, 2020.
- R. Lowe, Y. I. Wu, A. Tamar, J. Harb, O. Pieter Abbeel, and I. Mordatch, "Multi-agent actor-critic for mixed cooperative-competitive environments," *Advances in neural information processing systems*, vol. 30, 2017.
- J. Foerster, N. Nardelli, G. Farquhar, T. Afouras, P. H. Torr, P. Kohli, and S. Whiteson, "Stabilising experience replay for deep multi-agent reinforcement learning," in *International conference on machine learning*. PMLR, 2017, pp. 1146–1155.
- Y. Zhang, Z. Xu, Z. Wang, X. Yao, and Z. Xu, "Impacts of communication delay on vehicle platoon string stability and its compensation strategy: A review," *Journal of traffic and transportation engineering (English edition)*, 2023.
- S. Gronauer and K. Diepold, "Multi-agent deep reinforcement learning: a survey," *Artificial Intelligence Review*, vol. 55, no. 2, pp. 895–943, 2022.
- Y. Yan, B. Zhang, C. Li, and C. Su, "Cooperative caching and fetching in d2d communications-a fully decentralized multi-agent reinforcement learning approach," *IEEE Transactions on Vehicular Technology*, vol. 69, no. 12, pp. 16 095–16 109, 2020.
- C. Zhang, Q. Zhou, M. Hua, H. Xu, M. Bassett, and F. Zhang, "Cuboid equivalent consumption minimization strategy for energy management of multi-mode plug-in hybrid vehicles considering diverse time scale objectives," *Applied Energy*, vol. 351, p. 121901, 2023.
- M. Hua, C. Zhang, F. Zhang, Z. Li, X. Yu, H. Xu, and Q. Zhou, "Energy management of multi-mode plug-in hybrid electric vehicle using multi-agent deep reinforcement learning," *Applied Energy*, vol. 348, p. 121526, 2023.
- D. Chen, K. Zhang, Y. Wang, X. Yin, Z. Li, and D. Filev, "Communication-efficient decentralized multi-agent reinforcement learning for cooperative adaptive cruise control," *IEEE Transactions on Intelligent Vehicles*, 2024.
- M. Bando, K. Hasebe, A. Nakayama, A. Shibata, and Y. Sugiyama, "Dynamical model of traffic congestion and numerical simulation," *Physical review E*, vol. 51, no. 2, p. 1035, 1995.
- Q. Wang, H. Dong, F. Ju, W. Zhuang, C. Lv, L. Wang, and Z. Song, "Adaptive leading cruise control in mixed traffic considering human behavioral diversity," *IEEE Transactions on Intelligent Transportation Systems*, pp. 1–12, 2023.
- L. Guzzella, A. Sciarretta *et al.*, *Vehicle propulsion systems*. Springer, 2007, vol. 1.
- A. Abdi and F. Fekri, "Quantized compressive sampling of stochastic gradients for efficient communication in distributed deep learning," in *Proceedings of the AAAI Conference on Artificial Intelligence*, vol. 34, no. 04, 2020, pp. 3105–3112.
- A. Anesiadou, M. Makridis, B. Ciuffo, and K. Mattas, "Open acc database," *European Commission, Joint Research Centre (JRC) [Dataset]* PID: <http://data.europa.eu/89h/9702c950-c80f-4d2f-982f-44d06ea0009f>, 2020.
- S. Sukhbaatar, R. Fergus *et al.*, "Learning multiagent communication with backpropagation," *Advances in neural information processing systems*, vol. 29, 2016.